Electronic Supplementary Material (ESI) for Analytical Methods.

Supporting documents for:

Systematic optimization of a pyromellitic acid background electrolyte for capillary electrophoresis with indirect UV-Vis detection and online pre-concentration analysis of thiosalt anions in the treated mine tailings pond

Michael Pappoe, Christina S. Bottaro

In this section we present additional information on the UV-vs spectra of PMA (Figure S1), the influence of [TMAOH] on EOF and thiosalts separation efficiency (Figures S 2), of influence of [CTAB] on EOF and thiosalts separation efficiency (Figures S 3) and influence of [HMOH] on EOF and thiosalts separation efficiency (Figures S 4); influence of [PMA] on the sensitivity and separation efficiency of thiosalts species (Figure S 5), pH on the separation efficiency using the optimized PMA BGE (Figures S 6), influence of applied voltage on separation efficiency using optimized PMA BGE (Figures S 7); comparison of commercially available PMA BGE vs optimized PMA BGE under different applied voltage conditions (Figures S 8 and 9); effect of sampling stacking on sensitivity of analysis (Figure S 10); electropherogram of real thiosalts tailings pond sample and addition of thiosalts standards (Figure S 11, and standard addition calibration curves of thiosalts tailings pond sample (Figures S 12 - 16). Unless otherwise stated all migration times are in min.

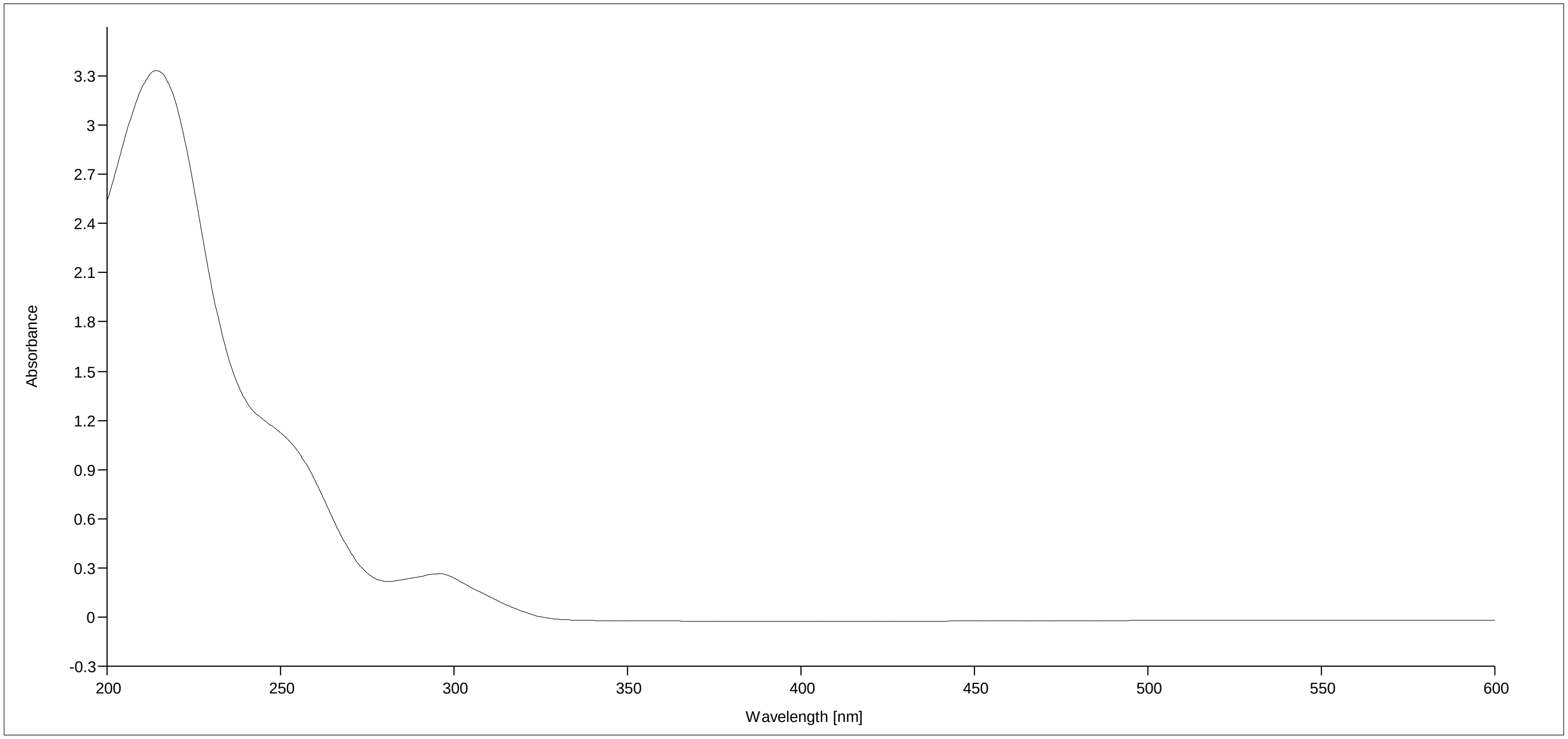

Figure S 1. UV-vis spectra of pyromellitic acid (PMA). [PMA] = 1.25 × 10^{-4} M, λ_{max} = 214 nm.

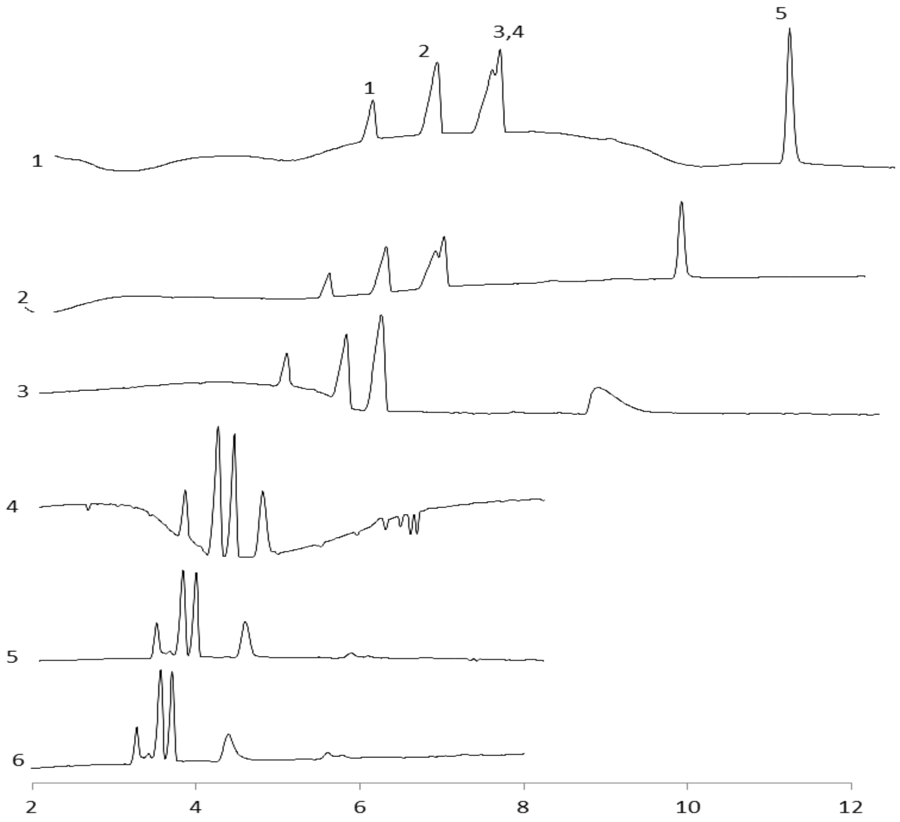

Time (min)

Figure S 2. Electropherogram showing the effect of increase in [TMAOH] on separation efficiency of 5 thiosalts species. 1. No TMAOH, 2. [TMAOH] = 0.20 mM, 3. [TMAOH] = 0.40, 4. [TMAOH] = 0.60 mM, 5. [TMAOH] = 0.80 mM, 6. [TMAOH] = 1.00 mM. CZE conditions: injection: 250 mbar.s, applied field: -20 kV, temperature: 25 °C, indirect UV detection at λ = 350 nm, Ref 200 nm. BGE 2.00 mM PMA pH adjusted to 8 with TEA.

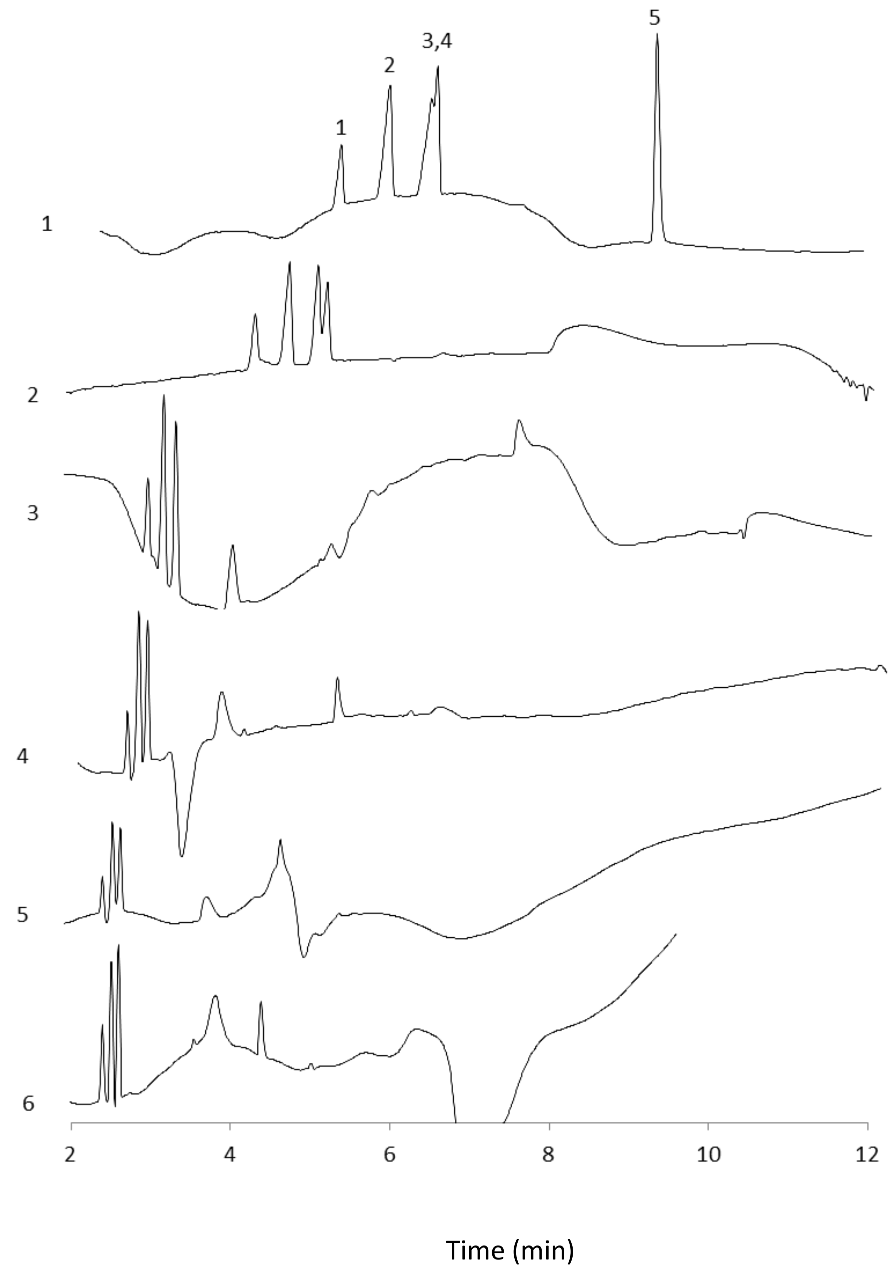

Figure S 3. Electropherogram showing the effect of increase in [CTAB] on separation efficiency of 5 thiosalts species. 1. [CTAB] = 0.00 mM, 2. [CTAB] = 0.20 mM, 3. [CTAB] = 0.40, 4. [CTAB] = 0.60 mM, 5. [CTAB] = 0.80 mM, 6. [CTAB] = 1.00 mM. CZE conditions: injection: 250 mbar.s, applied field: -20 kV, temperature: 25 ºC, indirect UV detection at λ = 350 nm, Ref 200 nm. BGE 2.00 mM PMA pH adjusted to 8 with TEA.

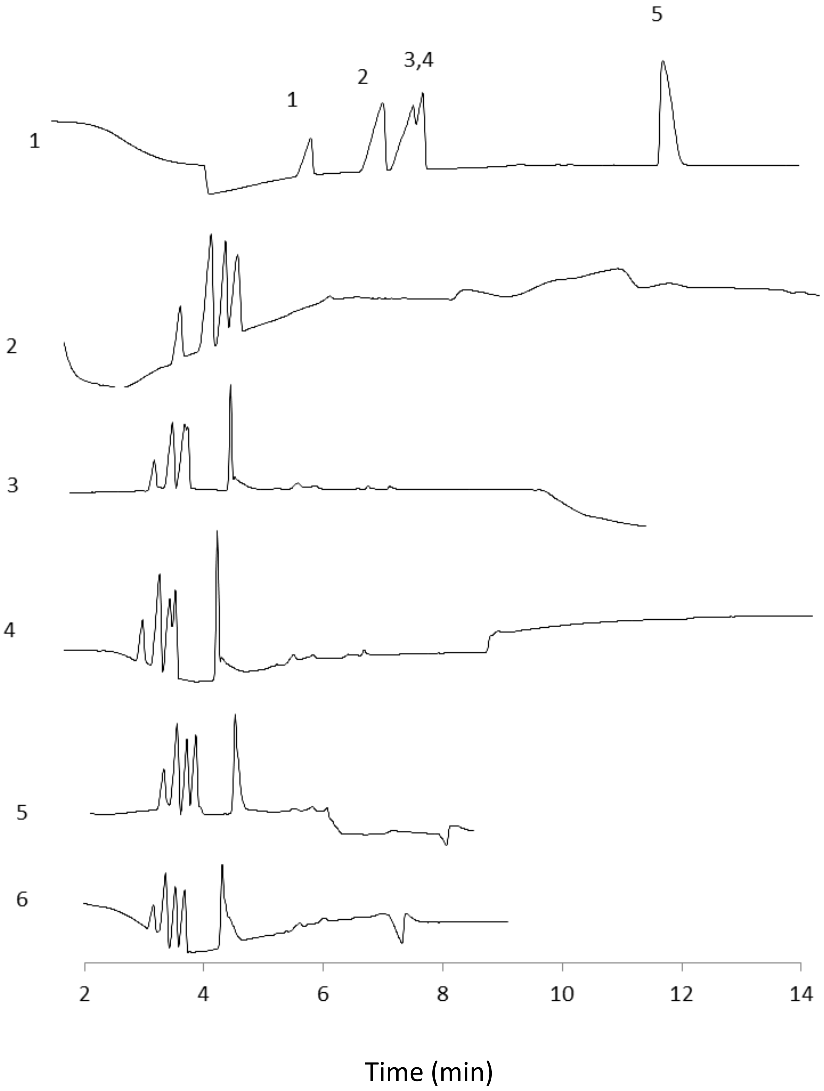

Figure S 4. Electropherogram showing the effect of increase in [HMOH] on separation efficiency of 5 thiosalts species. 1. [HMOH] = 0.00 mM, 2. [HMOH] = 0.20 mM, 3. [HMOH] = 0.40, 4. [HMOH] = 0.60 mM, 5. [HMOH] = 0.80 mM, 6. [HMOH] = 1.00 mM. CZE conditions: injection: 250 mbar.s, applied field: -20 kV, temperature: 25 °C, indirect UV detection at $\lambda = 350$ nm, Ref 200 nm. BGE 2.00 mM PMA pH adjusted to 8 with TEA.

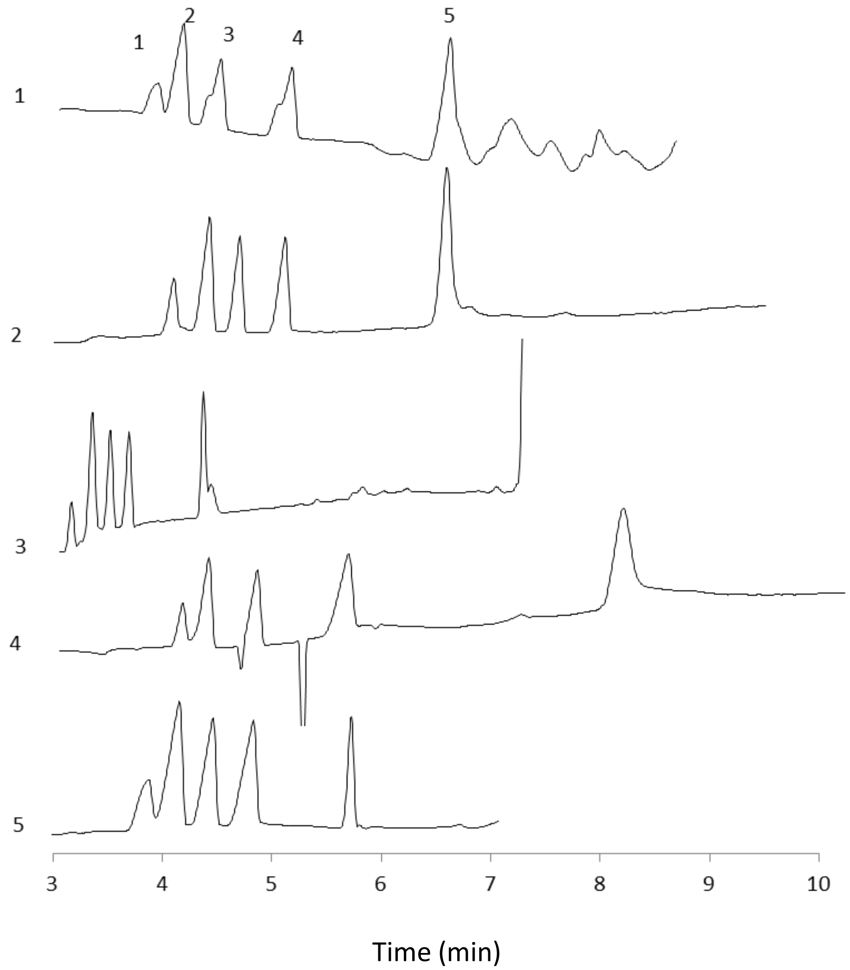

Figure S 5. Electropherogram showing the effect of increase in [PMA] on sensitivity and separation efficiency of 5 thiosalts species. 1. [PMA] = 1.00 mM, 2. [PMA] = 1.50 mM, 3. [PMA] = 2.00 mM, 4. [PMA] = 2.50 mM, 5. [PMA] = 3.00 mM. CZE conditions: injection: 250 mbar.s, applied field: -20 kV, temperature: 25 °C, indirect UV detection at $\lambda = 350$ nm, Ref 200 nm. BGE 0.80 mM HMOH with PMA pH adjusted to 8 with TEA.

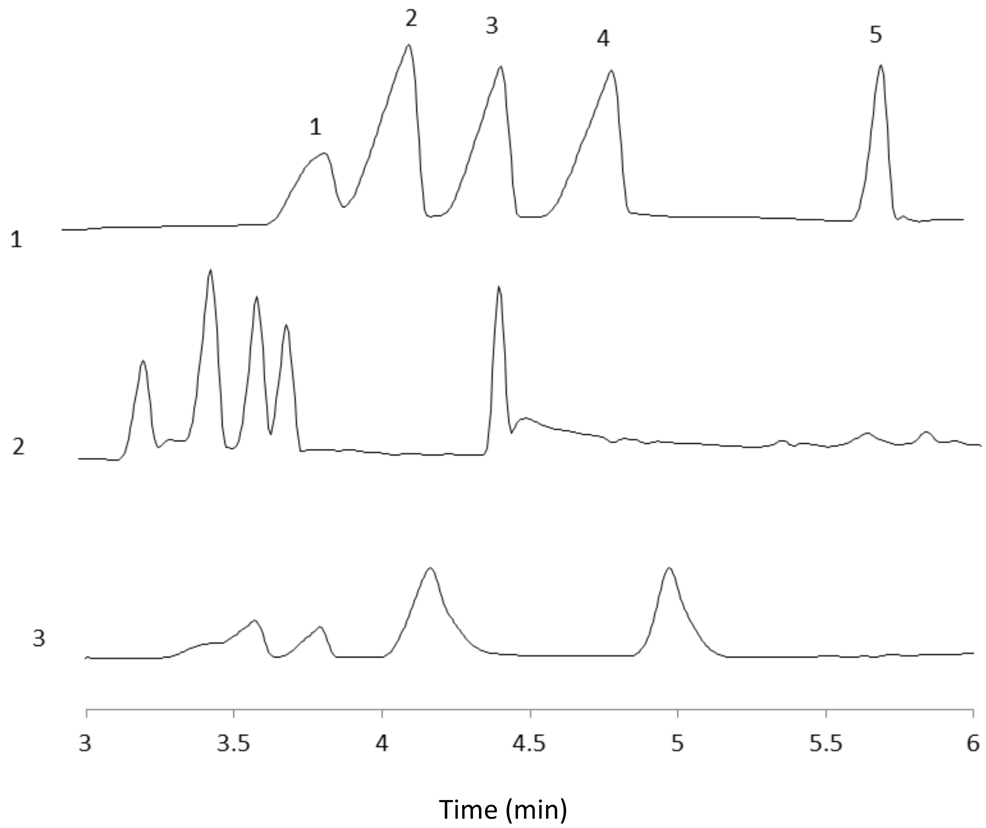

Figure S 6. Electropherogram showing the effect of increase in pH on sensitivity and separation efficiency of 5 thiosalts species. 1. pH = 7, 2. pH = 8, pH = 9 CZE conditions: injection: 250 mbar.s, applied field: -20 kV, temperature: 25 ºC, indirect UV detection at λ = 350 nm, Ref 200 nm. BGE [PMA] = 2.00 mM, [HMOH] = 0.80 mM pH adjusted to 7, 8 and 9 with TEA.

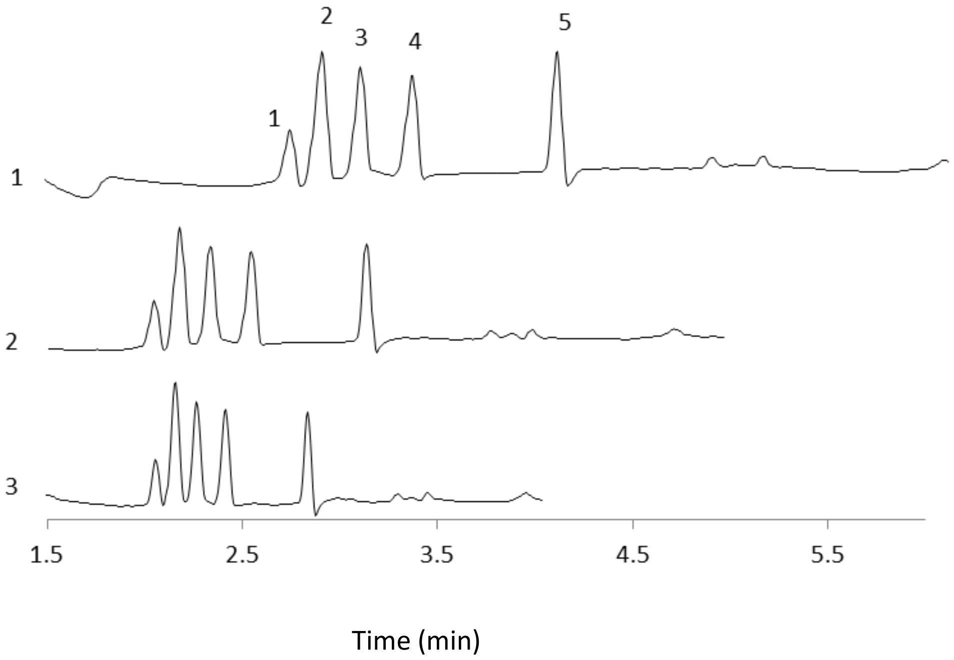

Figure S 7. Electropherogram showing the effect of increase in electric field strength on sensitivity and separation efficiency of 5 thiosalts species. 1. -20 kV, 2. -25 kV, 3. -30 kV CZE conditions: injection: 250 mbar.s, applied field: -20 kV, temperature: 25 ^{o}C, indirect UV detection at λ = 350 nm, Ref 200 nm. BGE [PMA] = 2.00 mM, [HMOH] = 0.80 mM pH adusted to with TEA.

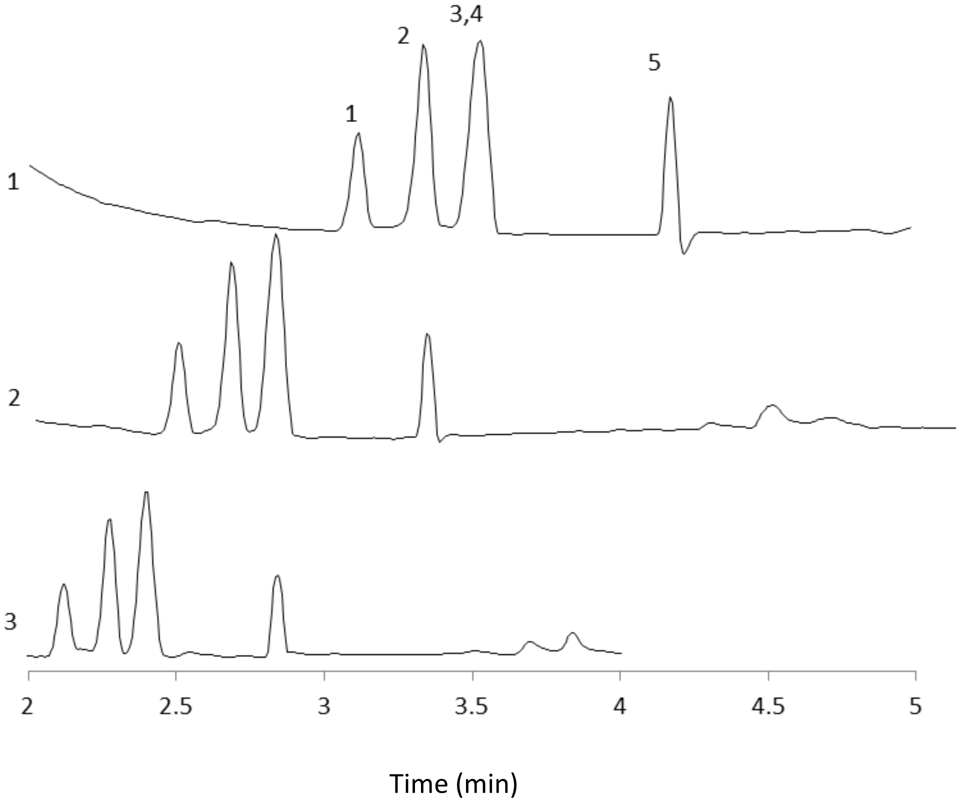

Figure S 8. Electropherogram showing the effect of increase in electric field strength on sensitivity and separation efficiency of 5 thiosalts species using commercially available PMA BGE. 1. -20 kV, 2. -25 kV, 3. -30 kV CZE conditions: injection: 250 mbar.s, applied field: -20 kV, temperature: 25 ^{o}C, indirect UV detection at $\lambda = 350$ nm, Ref 200 nm.

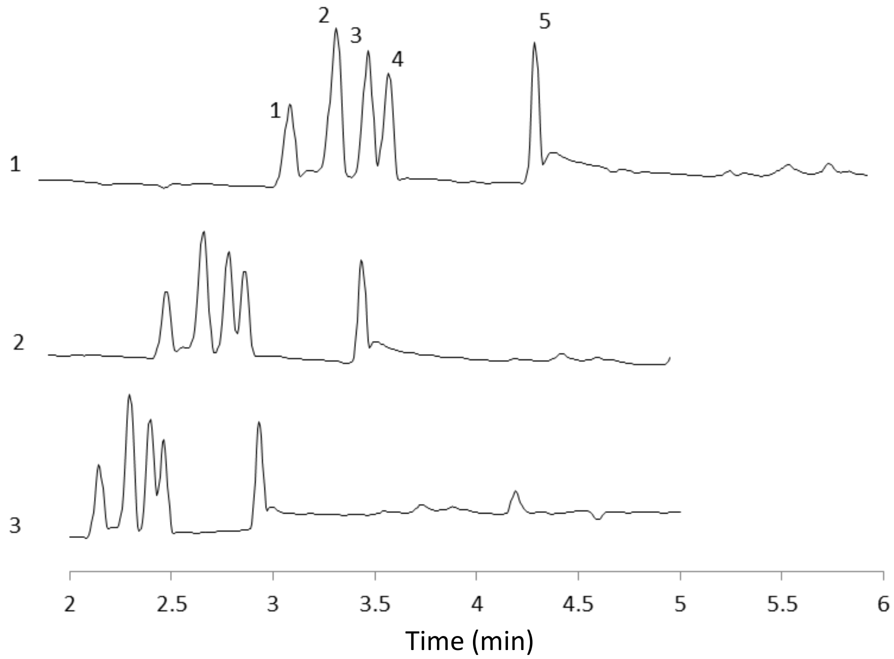

Figure S 9. Electropherogram showing the effect of increase in electric field strength on sensitivity and separation efficiency of 5 thiosalts species using the optimized PMA BGE.
1. -20 kV, 2. -25 kV, 3. -30 kV CZE conditions: injection: 250 mbar.s, applied field: -20 kV, temperature: 25 ^oC, indirect UV detection at λ = 350 nm, Ref 200 nm.

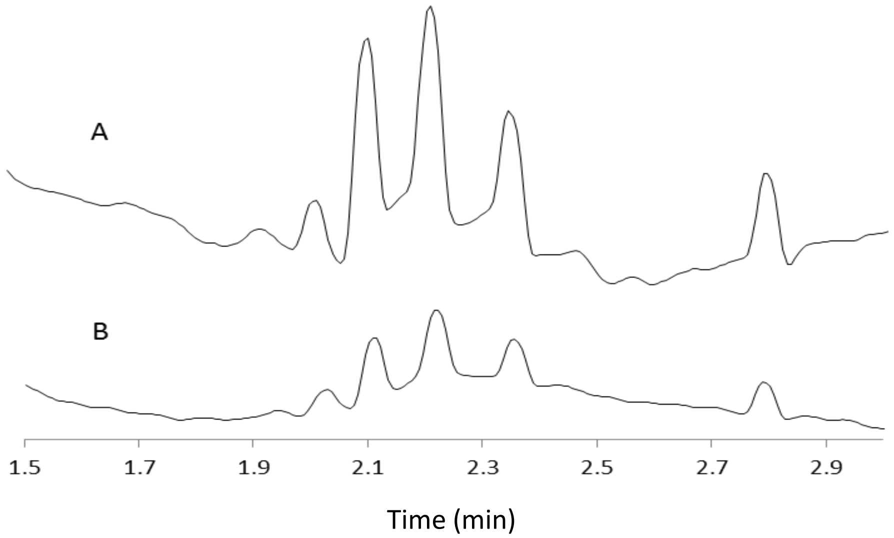

Figure S 10. Electropherogram of thiosalts showing the influence of FASS on detection sensitivity. A. Analysis with stacking 3s at 30 mbar of water followed by 5 s at 50 mbar of sample, B. Analysis without stacking. [thiosalts] = 0.2 µg/mL each.

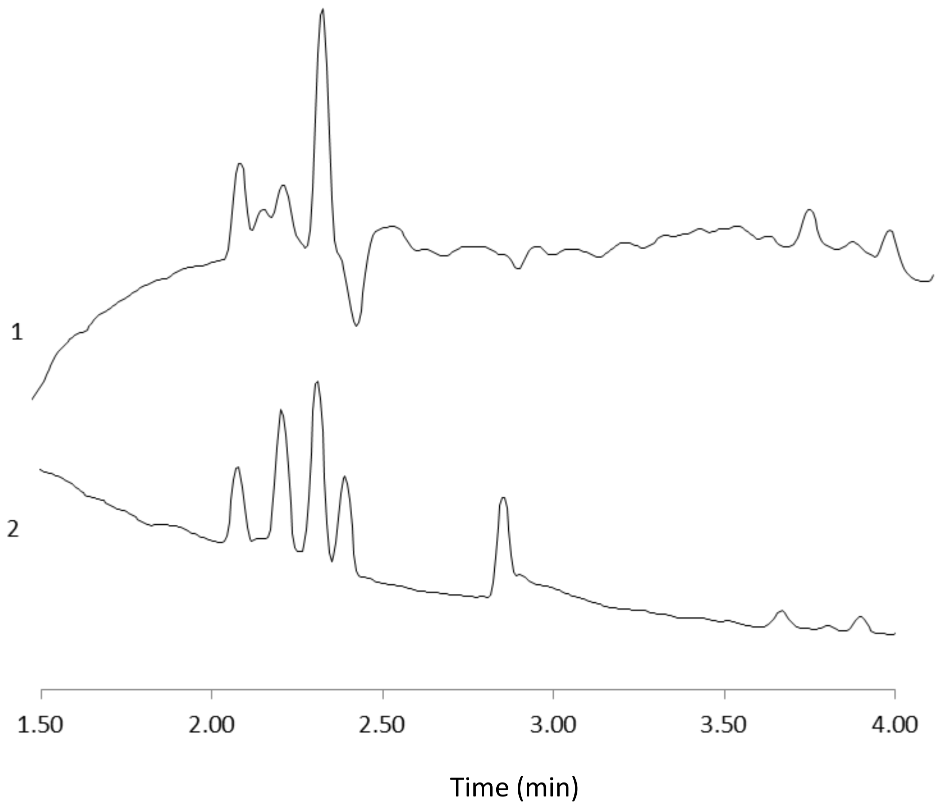

Figure S 11. Electropherograms of 1. Diluted (1:50) real sample from surface of thiosalts tailings pond, 2. Addition of 500 µL addition of thiosalt standard mixture 1 CZE conditions: injection: 250 mbar.s, applied field: -20 kV, temperature: 25 °C, indirect UV detection at λ = 350 nm, Ref 200 nm. BGE [PMA] = 2.00 mM, [HMOH] = 0.80 mM pH adjusted to with TEA.

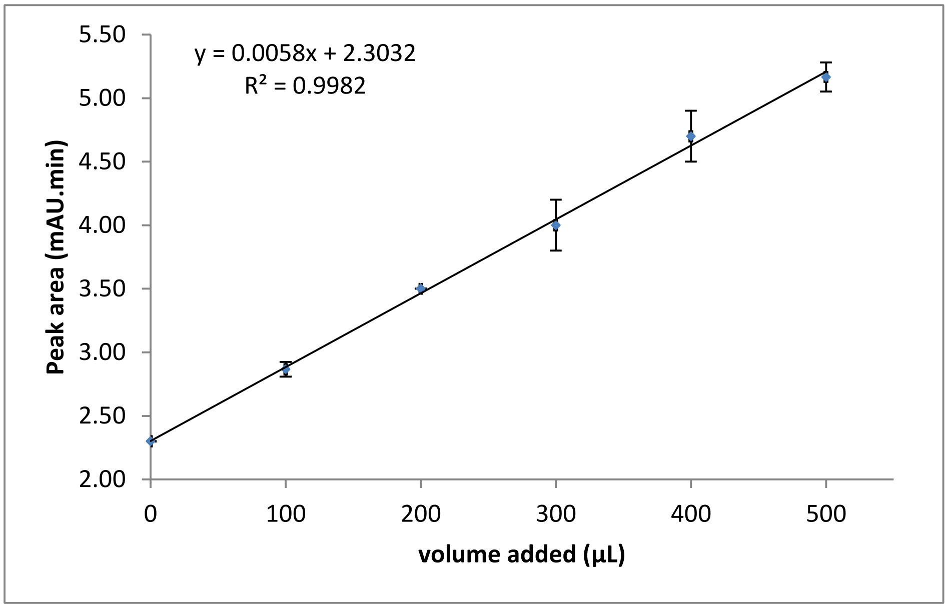

Figure S 12. Standard addition calibration curve showing the effect of addition of 0.33 µg/mL of sulfate standard to 1:100 diluted sample on the peak area of sulfate

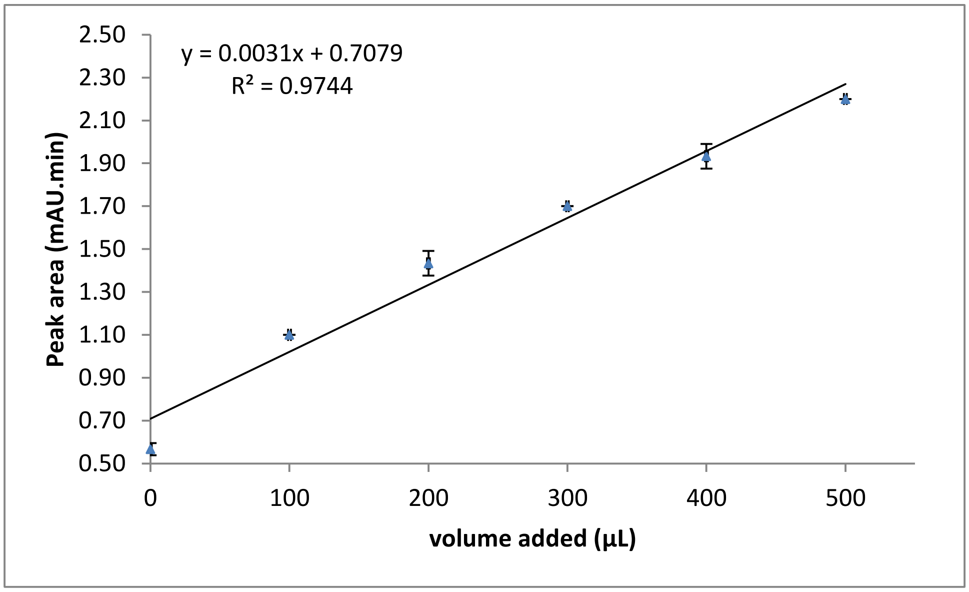

Figure S 13. Standard addition calibration curve showing the effect of addition of 0.45 µg/mL of thiosulfate standard to 1:100 diluted sample on the peak area of thiosulfate

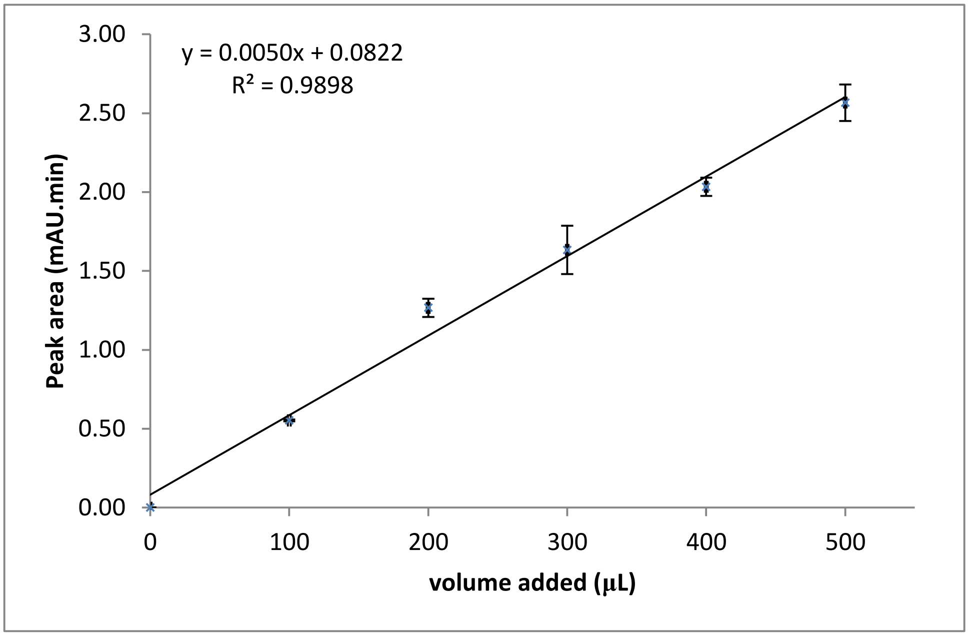

Figure S 14. Standard addition calibration curve showing the effect of addition of 0.88 µg/mL of trithionate standard to 1:50 diluted sample on the peak area of trithionate

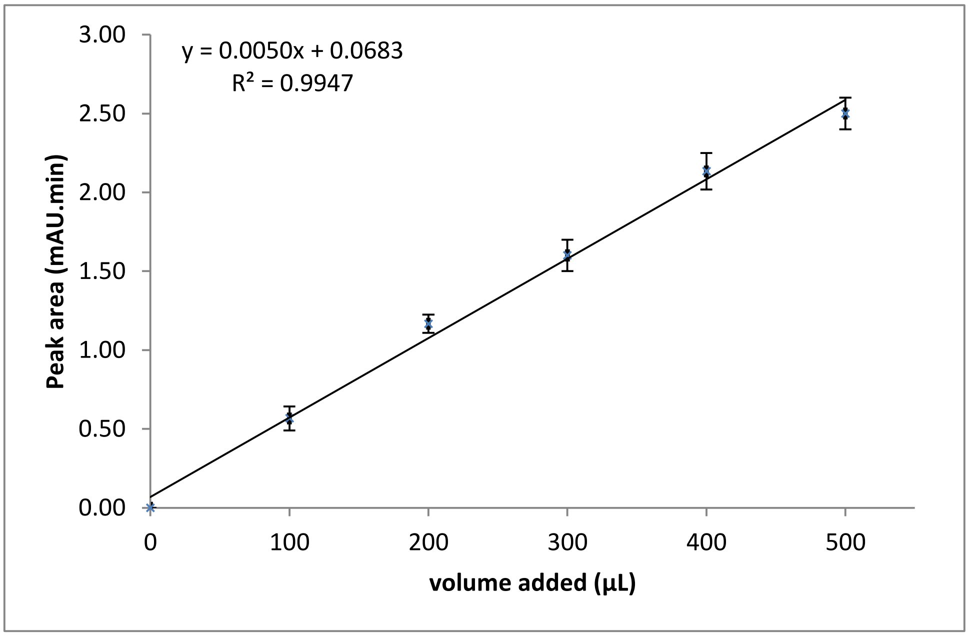

Figure S 15. Standard addition calibration curve showing addition of 0.88 µg/mL of tetrathionate standard to 1:100 diluted sample on the peak area of tetrathionate

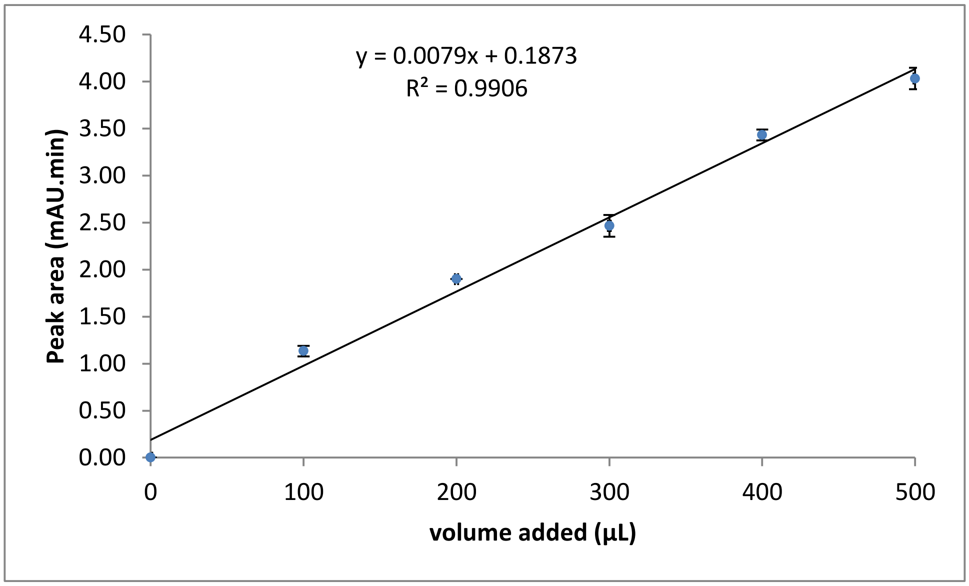

Figure S 16. Standard addition calibration curve showing addition of 0.88 μg/mL of pentathionate standard to 1:100 diluted sample on the peak area of pentathionate